

COMMUNICATION



Cite this: *Phys. Chem. Chem. Phys.*,
2014, 16, 22962

Received 16th July 2014,
Accepted 8th September 2014

DOI: 10.1039/c4cp03131h

www.rsc.org/pccp

Mechanical strain can switch the sign of quantum capacitance from positive to negative

Yuranan Hanlumyuang,^{†a} Xiaobao Li^{†b} and Pradeep Sharma^{*bc}

Quantum capacitance is a fundamental quantity that can directly reveal many-body interactions among electrons and is expected to play a critical role in nanoelectronics. One of the many tantalizing recent physical revelations about quantum capacitance is that it can possess a *negative* value, hence allowing for the possibility of *enhancing* the overall capacitance in some particular material systems beyond the scaling predicted by classical electrostatics. Using detailed quantum mechanical simulations, we found an intriguing result that mechanical strains can tune both *signs* and *values* of quantum capacitance. We used a small coaxially gated carbon nanotube as a paradigmatic capacitor system and showed that, for the range of mechanical strain considered, quantum capacitance can be adjusted from very large positive to very large negative values (in the order of plus/minus hundreds of attofarads), compared to the corresponding classical geometric value (0.31035 aF). This finding opens novel avenues in designing quantum capacitance for applications in nanosensors, energy storage, and nanoelectronics.

The behavior of nanoscale capacitors is remarkably rich and exhibits features unanticipated by conventional electrostatic theory.^{1–4} Intensive research has been recently ensued by materials development, elucidation of the fundamental science and applications related to nanocapacitors. Conventional wisdom, with its origins in textbook electrostatics, suggests that high capacitance can be achieved by reducing the characteristic size of the dielectric materials with high dielectric permittivity. For example, in the case of a thin film configuration, the classical electrostatic capacitance per unit area is taken to be $C_{\text{geo}} = \epsilon/d$ where ϵ is the dielectric permittivity and d is the thickness of the dielectric sandwiched between the electrodes. Accordingly, materials development has tended to focus on the selection and engineering of high dielectric

permittivity materials at the nanoscale level along with the concomitant challenges of their fabrication and testing. As the size of circuits reach nanoscale dimensions, the quantum nature of electronic devices can be utilized for the further miniaturization of electrical circuits. The capacitance of capacitors with thin dielectrics is also altered by quantum effects. In such devices, the capacitance consists of the well-known geometric value and another quantum contribution, called *quantum capacitance*.

Despite having been identified for nearly three decades,⁵ quantum capacitance (C_Q) has gained much interest only in recent years.^{6–9} Quantum capacitance arises from the finiteness of the density of states and the many-body interactions among electrons. It relates to the change in electron density with the chemical potential of the metallic gate. For a two-dimensional system, this relation is written as⁴

$$\frac{1}{C_Q} = \frac{d\mu/dn}{Ae^2}, \quad (1)$$

where contributions to $d\mu/dn$ stem from density of states and exchange/correlation energy functional of the gates. A is the area of the two-dimensional system. Since the appearance of C_Q requires only a finite $d\mu/dn$, it is ubiquitous. Considering different energetic contributions to the electron chemical potential μ , the quantum capacitance can then be separated into two components as⁴

$$\frac{1}{C_Q} = \frac{1}{C_{\text{DOS}}} + \frac{1}{C_{\text{XC}}}. \quad (2)$$

The capacitance C_{DOS} arises from the limiting density of states, given by $C_{\text{DOS}} = Ae^2\rho(E_F)$ or $C_{\text{DOS}} = Le^2\rho(E_F)$ in two- and one-dimensional systems, respectively. The symbol $\rho(E_F)$ represents the density of states (DOS) at the fermi level E_F . e is the electron charge. The many-body effects are lumped together as $1/C_{\text{XC}}$, in which both the exchange and correlation energy functionals are included. As discussed in ref. 4, the capacitance C_{XC} is negative.

Luryi has also reported that quantum capacitance depends on the electrical screening behaviors of the metallic gates.⁵

^a Department of Materials Engineering, Faculty of Engineering, Kasetsart University, Bangkok, 10900, Thailand

^b Department of Mechanical Engineering, University of Houston, TX, 77204, USA

^c Department of Physics, University of Houston, TX, 77204, USA.

E-mail: psharma@uh.edu; Fax: +1-713-743-4503; Tel: +1-713-743-4502

[†] These authors contributed equally to this work.

He studied a two-dimensional electron gas used as a grounded middle plate in a three-plate capacitor, and found that the two-dimensional gas, with small density of states (DOS), cannot completely screen the electric fields emanating from the top metallic gate. Clearly the laws of electrostatics, where complete electric-field screening is assumed, are not applicable in this system. In a simple metal–insulator–metal setup, the net capacitance (C_G) due to this screening effect, beyond the geometric value (C_{geo}), is written as

$$\frac{1}{C_G} = \frac{1}{C_{\text{geo}}} + \frac{2}{C_Q}, \quad (3)$$

where the magnitude of C_Q is usually much larger than that of C_{geo} , and it drops out as a contribution to C_G . The above expression shows that a system with low DOS tends to exhibit interesting effects since C_Q becomes comparable to the geometric capacitance.

Eqn (3) appears to suggest that the existence of C_Q tends to diminish the overall capacitance C_G . However, due to the negative exchange-correlation contribution, quantum capacitance can very well enhance the overall capacitance. Recently, a few materials systems have been identified in experiments as plausible realization of these enhancement effects. Examples include C–CuO₂–Cu coaxial nanowires and LaAlO₃–SrTiO₃ film systems where about 100% and 40% enhancement of capacitance has been reported, respectively.^{7,8}

A number of quantitative effects including the finite thickness of the capacitors and metal–insulator interface reconstruction among many others can influence quantum capacitance.⁴ We report here a surprising aspect of the quantum capacitance pertaining to mechanical deformation. This notion may be motivated by considering a two- or one-dimensional electron gas in the low-electronic density limit. A dimensionless distance r_s may be defined as $r_s = (\pi n_2 a^*)^{-1/2}$ or $r_s = (2n_1 a^*)^{-1}$ in two and one dimensions, respectively. The subscripts under carrier densities (n_2 and n_1) denote the dimensionality of the problem. a^* is the effective Bohr radius $a^* = \epsilon \hbar^2 / m^* e^2$. ϵ and m^* are the dielectric constant and the effective mass, respectively.^{10,11} In both cases, this distance characterizes the inter particle distances which directly depend on the amount of applied strain. Using this argument, we rationalize that mechanical strain should alter the electronic densities, and the exchange contribution to quantum capacitance. Many electron–mechanical coupling phenomena such as piezoelectricity^{12–14} and flexoelectricity,^{15,16} have been well studied for nanoscale materials. Also, strain effects on electronic density of states have been reported.¹⁷ Existing studies have already established the fundamental science underlying quantum capacitance.^{4,18–21} The potential role of mechanical effects remains largely unexplored, despite the study of sign-changing behavior of the quantum capacitance in the superconducting qubit–nanomechanical resonator systems.²²

In this paper, we explore the possibility of tuning quantum capacitance (hence the overall capacitance C_G) *via* mechanical strain. We find that, for a model system based on a carbon nanotube, in conjunction with appropriate doping levels, mechanical strain can indeed substantially change the values

of quantum capacitance and more intriguingly, switch its sign from positive to negative (and *vice versa*).

We used a small zigzag (10,0) carbon nanotube as a paradigmatic capacitive system. The nanotube was gated by a hollow metallic strip, and separated from the strip by an ideal SiO₂ insulator. In general, the low-dimensional nanotube has a small DOS value, and consequently cannot accumulate enough charge to completely screen the external field emanating from the metallic plates. The system is then ideal for studying quantum effects, beyond which the total screening is assumed. Indeed, it has already been reported that such a system with a coaxially gated nanotube possesses measurable quantum capacitance.²³

In this work, quantum capacitance was obtained using the nonequilibrium Green's function density functional tight-binding (DFTB) approach—the details related to the specific computational code may be found in ref. 24–26. It should be noted that though there is a bias applied through the cylindrical metallic gate, by treating the gate contact as a boundary condition for the electrostatic problem, the whole system always maintains equilibrium conditions. This approach is then appropriate for all equilibrium properties, such as capacitance, because the 'nonequilibrium' parts of the computational packages are not utilized. Our calculation details closely followed those given in ref. 23. The carbon–carbon interactions are those provided in the Slater–Koster parameter set in ref. 23 and PBC-0-1 ref. 27. The tight-binding Hamiltonian was evaluated self-consistently with the local charge fluctuation induced by the exchange of charges among atoms. The exchange and correlation (XC) functional was modeled using the local density approximation. In standard self-consistent DFTB, the second-order self-consistent charge extension relates to the Hubbard parameters as detailed in ref. 23, 28 and 29.

The nonequilibrium Green's function density functional DFTB package used^{24–26} was modified to allow for the coaxially gated (10,0) nanotube configuration. The underlying principles of the setup will become clear in a moment. Emphasizing first on the model configuration as shown in Fig. 1(a), the nanotube considered contained 2160 atoms and was about 22.6 nm in length. It was coaxially gated by a hollow metallic cylindrical strip located at a distance about 11.1 Å away. All features were placed inside a Poisson box where the electronic charge and potential were solved self-consistently. The separating insulator was SiO₂ with a relative permittivity of $\epsilon = 3.9$. The field lines through SiO₂ gave rise to the regular geometric capacitance (C_{geo}) as expected. Two metallic planes acted as grounded reference contacts which served as a source/drain of electrons in response to applied fields of the cylindrical gate. Dirichlet boundary conditions with zero potential were enforced on the metallic planes to simulate grounded contacts at the source and the drain. The same boundary conditions were also used to apply a constant voltage at the cylindrical metallic gate. The applied bias at the hollow metallic strip ($\delta V = 1$ mV) induced a net accumulation (or depletion) of charges on the surface of the nanotube. These charges were drawn from the source/drain outside of the Poisson box within the nonequilibrium Green's function treatment.

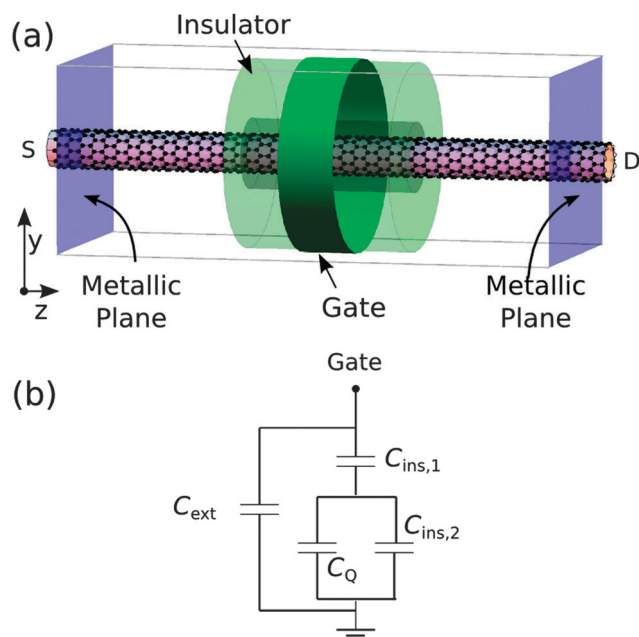


Fig. 1 (a) In a geometric setup for a nonequilibrium Green's function based on DFTB calculations, a zigzag (10,0) nanotube is located inside the Poisson box. The source and drain of electrons are marked by the letters S and D, respectively. (b) The circuit model of the cylindrically gated carbon nanotube.

As argued by Latessa *et al.*,^{23,30} the above approach allows one to extract information about the effects of exchange-correlation on quantum capacitance. We briefly summarize their findings here. Since it is well accepted that the exchange contribution to the total energy of a solid depends strongly on the number of charge carriers (also discussed in ref. 4), continuous *n*-doping of the nanotube tunes the number of charge carriers in the system, and consequently the exchange-correlation contributions. Here, doping is simulated by adjusting the number of fractional electrons in the valence orbital of each carbon atom. In this way, the number of electrons filling in the conduction subband can be tuned continuously. It will be clear in a moment how this continuous electron filling approach enables us to obtain useful information related to the effects of exchange-correlation on quantum capacitance.

The discussed model of an all-around gated nanotube can be simplified into an equivalent circuit model shown in Fig. 1(b). This circuit was obtained based on the seminal article by Luryi.⁵ The capacitance $C_{\text{ins},1}$ accounts for the field lines emanating from the cylindrical metallic gate to the nanotube surface, *i.e.* it represents the geometrical capacitance given by classical electrostatics. The capacitance $C_{\text{ins},2}$ quantifies the accumulated charge at the metallic plates inner to the nanotube. The capacitance $C_{\text{ins},2}$ arises from the *penetrating* field lines through the cylindrical surface of the nanotube to the artificial metallic planes near the ends of the tube. $C_{\text{ins},2}$ arises mainly because the nanotube having low density of states cannot accumulate enough electrons to screen all electric fields from the cylindrical metallic gate. These fields cause some charge accumulation on the metallic planes near and inner to

the tips of the nanotube. In this sense, $C_{\text{ins},2}$ is physical and arises due to our particular calculation setups. However, it should be noted that $C_{\text{ins},2}$ is not quantum capacitance, since it does not account for charge accumulation/depletion at the surface of the low-dimensional nanotube. Lastly, the capacitance (C_{ext}) in parallel to the main circuit accounts for possible charge accumulation at the metallic planes outer to the nanotube.

In addition to $C_{\text{ins},1}$, $C_{\text{ins},2}$, and C_{ext} , a bias at the cylindrical metallic gate may cause some charge accumulation/depletion on the nanotube surface due to the aforementioned electrical screening properties. This phenomenon leads to the extraneous quantum capacitance. C_Q may have either (a) negative, (b) zero, or (c) positive value depending on the density of charge carriers in the system. These different regimes correspond to (a) over-screening, (b) complete screening, or (c) partial screening of the nanotube in response to the bias at the cylindrical gate.^{18,23,30} In case (a), the nanotube overcompensates the gate field and accumulates more electrons than needed, leading to *negative* potential in the interior of the tube. In case (b), the accumulated charge on the nanotube surface completely screens the gate field, *i.e.* zero electrical potential is present at the center of the nanotube interior. Lastly, in case (c) the charge accumulation on the nanotube surface is limited by the density of states,⁵ and consequently the nanotube only partially screens the positive gate field. A small positive potential is then present in the interior of the nanotube. The numerical values of $C_Q(n)$ as a function of carrier density can be straightforwardly obtained after establishing relations between electrostatic potential profiles and doping levels *n*. Fig. 2 shows three regimes of potential profiles along the *y*-direction (shown in Fig. 1) where the carrier densities are (a) $n = 0.1033 \text{ \AA}^{-1}$, (b) 0.1005 \AA^{-1} , and (c) 0.0478 \AA^{-1} , respectively, and the applied gate voltage is $\delta V_G = 1 \text{ mV}$.

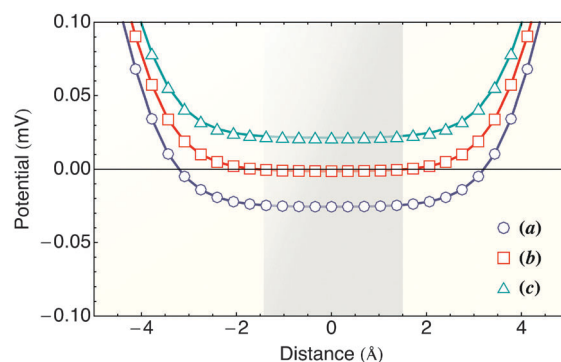


Fig. 2 Electrostatic potentials along the *y*-direction of a mechanically neutral (10,0) nanotube. The tube is outlined in the central shaded area. Three screening regimes, depending on carrier densities, are illustrated. (a) For $n = 0.1033 \text{ \AA}^{-1}$, the nanotube overcompensates the gate field and accumulates more electrons than needed, leading to *negative* potential in the interior of the tube, *i.e.* the nanotube *overscreen* the applied electric fields. (b) For $n = 0.1005 \text{ \AA}^{-1}$, the accumulated charge on the nanotube completely screens the gate field. Zero screened potential is present at the center of the nanotube interior. (c) At the carrier density $n = 0.0478 \text{ \AA}^{-1}$, the charge accumulation on the nanotube is limited by the density of states,⁵ and consequently the nanotube only partially screens the positive gate field. A small positive potential is then present in the interior of the nanotube.

The proceeding paragraphs and the accompanying figures make it clear that the rather specific geometric setup of the nanotube, insulator, metallic gate and metallic planes allows for direct calculations of C_Q . Taking advantage of the three screening regimes and the circuit model shown in Fig. 1(b), the quantum capacitance $C_Q(n_1)$ was obtained by computing the number of induced charge as a function of the carrier densities. By numerically evaluating the charge induced on the metallic planes shown in Fig. 1(a), we found that both $C_{\text{ins},2}$ and C_{ext} for all current long CNTs studied are negligible. The gate capacitance in the circuit model shown in Fig. 1(b) hence reduces to $1/C_G = 1/C_Q + 1/C_{\text{ins},1}$. In the case of complete screening, we have $1/C_G = 1/C_{\text{ins},1} = \delta V_G / \delta Q(n_{1,\text{crit}})$, whereas for partial screening or overscreening $1/C_G = 1/C_{\text{ins},1} + 1/C_Q(n_1) = \delta V_G / \delta Q(n_1)$. Since the gate voltage is externally controlled, δV_G in both cases can be equated to yield the quantum capacitance as

$$C_Q(n_1) = C_{\text{ins},1} \left[\frac{\delta Q(n_{1,\text{crit}})}{\delta Q(n_1)} - 1 \right]^{-1}, \quad (4)$$

where $n_{1,\text{crit}}$ is the critical value of the carrier densities when complete screening is observed. The task of computing quantum capacitance then reduces to determining $n_{1,\text{crit}}$ and the induced charge at each doping level. Here, an additional numerical optimizing routine has been implemented in coordination with the nonequilibrium Green's function DFTB package^{24–26} in order to obtain the induced charges. This numerical routine appropriately sets Fermi levels, necessary for integrating the energy subbands for charge densities. A necessary condition to determine the Fermi levels is the charge neutrality. The charge tolerance in the Fermi energy optimizing routine is set to $\delta Q = 10^{-7}$ a.u. After obtaining appropriate Fermi energies, the nonequilibrium Green's function routine is then utilized to draw electrons from the source and the drain onto the cylindrical surface of the nanotube.^{25,26} Using this approach, we were able to verify our numerical quantum capacitance and potential profiles (Fig. 2) against the results in ref. 23.

After benchmarking our calculated quantum capacitance at zero strain, obtaining the effects of uniaxial strain on the quantum capacitance is straightforward. Small uniaxial stretch and compression can be applied to the nanotube using the relation $z \mapsto (1 + \varepsilon)z$. Quantum capacitances at three strain levels are shown in Fig. 3. The carrier density is measured in the unit, electron charge per compressed/stretched area. As well-evident from the figure, for an appropriate doping level, C_Q can change both its sign and magnitude depending on the level of applied mechanical strain. For example at the carrier density of about 0.10 \AA^{-1} , C_Q changes from a very high positive value at the $\varepsilon = -0.3\%$ to about $C_Q \approx -5 \text{ aF}$ at $\varepsilon = 1.5\%$. For the (10,0) nanotube considered, this change in C_Q accounts for about a 10% change in the overall capacitance C_G in the classical complete screening case. Computed from expressions leading eqn (4), the classical capacitance is $C_{\text{ins},1} = 0.31035 \text{ aF}$. The dashed lines are the corresponding capacitance values calculated from $C_{\text{DOS}} = e^2 \rho(E_F) L$, i.e. the limiting DOS contribution to the quantum capacitance.

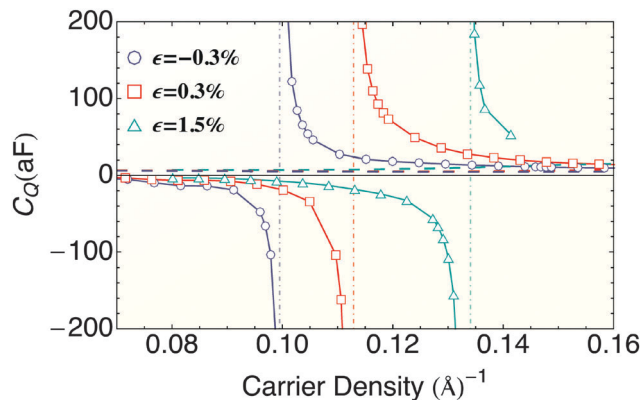


Fig. 3 The effect of strain on quantum capacitance. The carrier density on the horizontal axis is in the unit, electron per physical (strained) area. A solid line with triangle, square and circle indicates the quantum capacitance at 1.5%, 0.3% and -0.3% strain, respectively. The dashed line indicates the C_{DOS} at 1.5%, 0.3% and -0.3% strain, respectively.

The change in sign at the carrier density $n = 0.10 \text{ \AA}^{-1}$ can be interpreted as follows. Recall that the quantum capacitance consists of two contributions, the DOS and the exchange-correlation terms, as $1/C_Q = 1/C_{\text{XC}} + 1/C_{\text{DOS}}$. The sign switching occurs when the negative term $1/C_{\text{XC}}$ compensates the positive term $1/C_{\text{DOS}}$.⁴ Evidently from Fig. 3, C_{DOS} does not deviate much across the range of strain considered ($\varepsilon = -0.3\%$ to 1.5%). The band diagrams shown in Fig. 4 at different strain levels further support this point. Therefore, it is reasonable to conclude that C_Q undergoes a sign change mainly because of the variation in the exchange-correlation contribution. As the level of strains goes from small compression to tensile, the electronic density decreases due to an increase in the cylindrical tube area. At a sufficiently low electron density, the exchange-correlation contribution C_{XC} dominates C_{DOS} , producing a negative quantum capacitance.

The quantum capacitance of a one-dimensional nanowire is related to the second derivative of the exchange energy with respect to the inter-particle distance r_s as $1/C_{\text{X}} \propto n_1 r_s^2 d^2 E_{\text{X}} / dr_s^2$.¹⁰

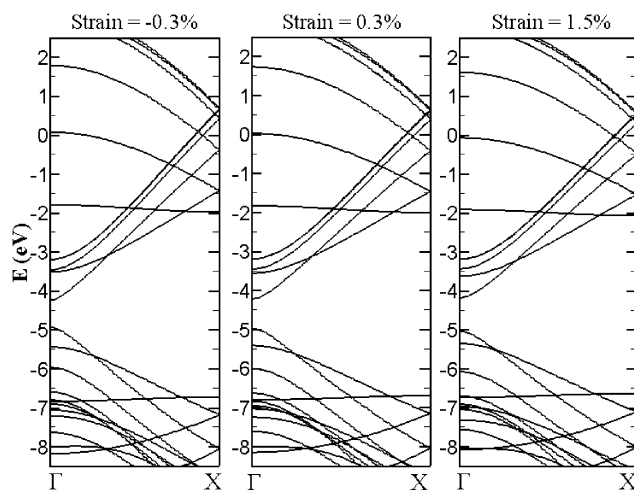


Fig. 4 Dependence of CNT band diagrams on mechanical strain.

Therefore, it is reasonable to postulate that our observed sign switching is also caused due to this change in the energy curvature. Though we have not rigorously proved this strain-exchange/correlation relation, our numerical results support this postulate. To establish rigorously underlying principles to the sign-changing behavior of $n_1 r_s^{-2} d^2 E_{XC}/dr_s^2$ under different mechanical loads remains an interesting new research avenue.

The link between the mechanical strain and the curvature of the exchange energy can also be established considering a simple analysis. Approximating the (10,0) nanotube of radius R_0 as a solid dielectric cylinder, its dielectric constant is given by $\epsilon_{||} = 1 + 4\alpha_{||}/R_0^2 \approx 38$, where $R_0 = 3.914 \text{ \AA}$ and $\alpha_{||} = 142 \text{ \AA}^2$ is the longitudinal polarizability per unit length.³¹ Taking the effective mass of the electron as $m^* = sm_e$, the effective Bohr radius is $a^* = (\epsilon_{||}/s)a_B \approx 243 \text{ \AA}$, where $a_B = \hbar^2/m_e e^2$. For the range of carrier density from $n_1 = 0.16 \text{ \AA}^{-1}$ to $n_1 = 0.04 \text{ \AA}^{-1}$ in this study, the corresponding inter-particle distances are $r_s = 0.01 \ll 1$ and $r_s = 0.05 \ll 1$, respectively. Using the local-field correction within a sum-rule approach, Calmels and Gold have shown that in the regime $r_s \ll 1$ the exchange energy per particle of a quasi-1D nanowire has an asymptotic form:³²

$$E_X(n_1) \sim -\frac{a^*}{R_0} \left[2.4082 + \frac{18}{5\pi} c r_s \left(\ln \frac{c r_s}{2} - \frac{1}{2} \right) \right], \quad (5)$$

where $c = 4g_v a^*/\pi R_0$ and g_v is the valley degeneracy. Consequently, the energy curvature at $r_s = r_s^0$ is

$$\left. \frac{d^2 E_X}{dr_s^2} \right|_{r_s=r_s^0} \sim -\frac{18ca^*}{5\pi R_0 r_s^0}, \quad \text{for } r_s^0 \ll 1. \quad (6)$$

Making an approximation that the mechanical strain alters the inter-particle distance as $r_s^0 \mapsto r_s^0(1 + \epsilon)$, for small strain $d^2 E_X/dr_s^2 \sim - (18ca^*/5\pi R_0 r_s^0)(1 - \epsilon + \dots)$. That is, in the limit $r_s \ll 1$ (as in our present study), the exchange energy curvature $d^2 E_X/dr_s^2$ depends linearly on the mechanical strain. Similarly, the variation of the correlation energy curvature with the strain is anticipated.

In summary, we have explored the notion of switching the sign of quantum capacitance *via* mechanical strain, using a coaxially gated carbon nanotube as a model material system. From full electronic structure calculations within density functional tight-binding theory, it is clear that the interplay between doping and exchange-correlation energy functional plays a crucial role in determining both the sign and magnitude of quantum capacitance. Fig. 3 clearly demonstrates that the quantum capacitance can be mechanically controlled from very large positive to very large negative values. It is then natural to ask if this nanotube property can be utilized in the nanosensing technology. A possible experiment to detect such a large negative/positive quantum capacitance is to modify the ingenious apparatus, as reported in ref. 33. A pair of graphene could be used as two quantum wells separated by some small distance. Both graphene sheets could be deposited on a piezoelectric material to simulate strains, while small gates can be intentionally attached to add/remove electrons to the system. Strong signals due to the ratio between differential change in gate electric field and the penetrating fields ought to be observed.

As discussed in ref. 33, the ratio correlates directly to quantum capacitance. Lastly, it should be emphasized that the concept of quantum capacitance is not limited only to carbon nanotubes. Exploring the mechanical effects in other material systems, such as BN monolayers and $\text{LaAlO}_3/\text{SrTiO}_3$ films, could very well open new avenues in improving lower-power devices and in energy storage for nanoelectronics. Moreover, the switching of sign promises a novel “quantum sensing” mechanism.

Acknowledgements

YH and XL acknowledge useful correspondences with Alessandro Pecchia, Aldo Di Carlo, Bálint Aradi and Gabriele Penazzi during the course of this work. Funding is gratefully acknowledged from the M. D. Anderson Professorship, NSF CMMI-0969086 and NSF CMMI-1161163. YH also gratefully acknowledges support through the Faculty of Engineering, Kasetsart University (Thailand).

References

- 1 M. Büttiker, *J. Phys.: Condens. Matter*, 1993, **5**, 9361.
- 2 M. Stengel and N. A. Spaldin, *Nature*, 2006, **443**, 679.
- 3 M. Stengel, D. Vanderbilt and N. A. Spaldin, *Nature*, 2009, **8**, 392.
- 4 T. Kopp and J. Mannhart, *J. Appl. Phys.*, 2009, **106**, 064504.
- 5 S. Luryi, *Appl. Phys. Lett.*, 1988, **52**, 501.
- 6 S. Ilani, L. A. K. Donev, M. Kindermann and P. L. McEuen, *Nat. Phys.*, 2006, **2**, 687.
- 7 L. Li, C. Richter, S. Paetel, T. Kopp, J. Mannhart and R. C. Ashoori, *Science*, 2011, **332**, 825.
- 8 Z. Liu, Y. Zhan, G. Shi, S. Moldovan, M. Gharbi, L. Song, L. Ma, W. Gao, J. Huang, R. Vajtai, F. Banhart, P. Sharma, J. Lou and P. M. Ajayan, *Nat. Commun.*, 2012, **3**, 1.
- 9 G. L. Yu, R. Jalil, B. Belle, A. S. Mayorov, P. Blake, F. Schedin, S. V. Morozov, L. A. Ponomarenko, F. Chiappini, S. Wiedmann, U. Zeitler, M. I. Katsnelson, A. K. Geim, K. S. Novoselov and D. C. Elias, *Proc. Natl. Acad. Sci. U. S. A.*, 2013, **110**, 3282.
- 10 L. Calmels and A. Gold, *Phys. Rev. B: Condens. Matter Mater. Phys.*, 1996, **53**, 10846.
- 11 B. Skinner and B. I. Shklovskii, *Phys. Rev. B: Condens. Matter Mater. Phys.*, 2010, **82**, 155111.
- 12 M. Zelisko, Y. Hanlumuang, S. Yang, Y. Liu, C. Lei, J. Li, P. M. Ajayan and P. Sharma, *Nat. Commun.*, 2014, **5**, 4284.
- 13 N. Sai and E. J. Mele, *Phys. Rev. B: Condens. Matter Mater. Phys.*, 2003, **68**, 241405(R).
- 14 K. A. N. Duerloo, M. T. Ong and E. J. Read, *J. Phys. Chem. Lett.*, 2012, **3**, 2871–2876.
- 15 T. Dumitrica, C. M. Landis and B. I. Yakobson, *Chem. Phys. Lett.*, 2002, **360**, 182–188.
- 16 T. D. Nguyen, S. Mao, Y.-W. Yeh, P. K. Purohit and M. C. McAlpine, *Adv. Mater.*, 2013, **25**, 946–974.
- 17 H. C. Hwang, A. Sher and C. Gross, *Phys. Rev. B: Solid State*, 1976, **13**, 4237–4244.
- 18 G. F. Giuliani and G. Vignale, *Quantum Theory of the Electron Liquid*, Cambridge University Press, Cambridge, 2005.

- 19 M. M. Fogler, *Phys. Rev. Lett.*, 2005, **94**, 056405.
- 20 S. K. Kusminskiy, J. Nilsson, D. K. Campbell and A. H. Castro Neto, *Phys. Rev. Lett.*, 2008, **100**, 106805.
- 21 G. Borghi, M. Polini, R. Asgari and A. H. MacDonald, *Phys. Rev. B: Condens. Matter Mater. Phys.*, 2010, **82**, 155403.
- 22 S. N. Shevchenko, S. Ashhab and F. Nori, *Phys. Rev. B: Condens. Matter Mater. Phys.*, 2012, **85**, 094502.
- 23 L. Latessa, A. Pecchia and A. Di Carlo, *Phys. Rev. B: Condens. Matter Mater. Phys.*, 2005, **72**, 035455.
- 24 B. Aradi, B. Hourahine and Th. Frauenheim, *J. Phys. Chem. A*, 2007, **111**, 5678.
- 25 A. Pecchia and A. Di Carlo, *Rep. Prog. Phys.*, 2004, **67**, 1497.
- 26 A. Di Carlo, A. Pecchia, L. Latessa, Th. Frauenheim and G. Seifert, *Introducing Molecular Electronics*, chapter Tight-Binding DFT for Molecular Electronics (gDFTB), Springer, 2005, p. 153.
- 27 E. Rauls, R. Gutierrez, J. Elsner and Th. Frauenheim, *Solid State Commun.*, 1999, **111**, 459.
- 28 T. Frauenheim, G. Seifert, M. Elstner, T. Niehaus, C. Köhler, M. Amkreutz, M. Sternberg, Z. Hajnal, A. D. Carlo and S. Suhai, *J. Phys.: Condens. Matter*, 2002, 3015.
- 29 M. Elstner, D. Porezag, G. Jungnickel, J. Elsner, M. Haugk, T. Frauenheim, S. Suhai and G. Seifert, *Phys. Rev. B: Condens. Matter Mater. Phys.*, 1998, **58**, 7260.
- 30 L. Latessa, A. Pecchia and A. Di Carlo, *IEEE Trans. Nanotechnol.*, 2007, **6**(1), 13–21.
- 31 B. Kozinsky and N. Marzari, *Phys. Rev. Lett.*, 2006, **96**, 166801.
- 32 L. Calmels and A. Gold, *Phys. Rev. B: Condens. Matter Mater. Phys.*, 1995, **52**(15), 10841.
- 33 J. P. Eisenstein, L. N. Pfeiffer and K. W. West, *Phys. Rev. Lett.*, 1992, **68**(5), 674.